Determination of mass-loss rates of PG 1159 stars from FUV spectroscopy

Lars Koesterke[1]

Institut für Physik, Astrophysik, Universität Potsdam, Am Neuen Palais 10, D-14469 Potsdam, Germany

and

Klaus Werner[1]

Institut für Astronomie und Astrophysik, Universität Tübingen, Waldhäuser Straße 64, D-72076 Tübingen, Germany

Received ______________; accepted ______________

To appear in The Astrophysical Journal Letters

[1]ORFEUS-SPAS II Guest Investigator

ABSTRACT

We determine mass-loss rates of four hot, low-gravity PG 1159 stars which are regarded as immediate descendants of Wolf-Rayet central stars of planetary nebulae (i.e. early spectral type [WCE]). The sample consists of classical hydrogen-deficient PG 1159 stars (K 1-16, NGC 246, RX J2117.1+3412) as well as one object of the very rare "hybrid" subtype which also exhibits hydrogen lines (NGC 7094). The sample is complemented by the famous [WC]–PG 1159 transition object Abell 78. Our analysis is based on the O VI 1032/1038Å resonance line which is the strongest wind-feature in these objects. FUV observations were performed with the Berkeley spectrograph during the ORFEUS-SPAS II mission. One spectrum is taken from archive data of the ORFEUS-SPAS I mission and another one was obtained with the Hopkins Ultraviolet Telescope during the Astro-2 mission. We find mass-loss rates ranging between $\log(\dot{M}/\mathrm{M}_\odot\mathrm{yr}^{-1}) = -8 \ldots -7$, as compared to the [WCE] stars which have mass-loss rates of about $\log(\dot{M}/\mathrm{M}_\odot\mathrm{yr}^{-1}) = -5.5 \ldots -6.5$. By comparison with theory we conclude that the wind of PG 1159 stars is driven by radiation pressure.

Subject headings: stars: AGB and post-AGB — stars: atmospheres — stars: evolution — stars: mass-loss — stars: chemically peculiar — ultraviolet: stars

1. Introduction

Roughly 20% of all hot post-AGB stars are hydrogen-deficient. The origin of this phenomenon is unclear, hence the existence of a considerable fraction of post-AGB stars remains still unexplained by standard stellar evolution theory. Basically, these H-deficient objects fall into two distinct spectral types, namely the Wolf-Rayet central stars of planetary nebulae (i.e. spectral type [WC]) and the further evolved PG 1159 stars, which in every other case are associated with a planetary nebula. The optical stellar spectra of both groups are dominated by He II lines and highly excited carbon and oxygen features (C IV and O VI). These lines are strong and purely in emission in the spectra of [WC] stars as they form in a fast, dense wind. In contrast the PG 1159 stars have weak and pure absorption line spectra, aside from very few emission lines whose nature is readily explained by non-LTE effects in static photospheres. During the recent years we have performed spectral analyses of the majority of [WC] and PG 1159 stars (Hamann 1997, Werner et al. 1997). It is now well established that both spectral classes form an evolutionary sequence. The [WC] stars roughly range between $T_{\rm eff}$=30 kK and 140 kK in the high-luminosity region of early post-AGB evolution. Mass-loss rates are high ($\log(\dot{M}/{\rm M}_{\odot}{\rm yr}^{-1}) = -5.5 \ldots -6.5$) and generally decrease with increasing $T_{\rm eff}$. Beginning at the hot end of the [WC] domain we find the PG 1159 stars continuing to even higher temperatures. They mark the hottest stages of post-AGB evolution as well as the stages of the subsequent luminosity decrease and cooling until the hot end of the white dwarf cooling sequence is entered. Realistic estimates of mass-loss rates of PG 1159 stars were lacking until these days.

For a detailed analysis we have selected a number of PG 1159 stars whose location in the HRD is closest to their [WC] progenitors (see Fig. 1). In spite of their close neighborhood it seems somewhat surprising that the optical spectra of these luminous PG 1159 stars look so entirely different from the [WCE] stars. Does this mean that the strongly different spectral appearance is a consequence of the fact that mass-loss rates decrease drastically within a very short evolutionary phase? As a key object to answer this question we included Abell 78 in our analysis, which besides Abell 30 is the only known [WC]–PG 1159 transition object, displaying a mixed emission/absorption line spectrum. UV spectroscopy is necessary for our purpose. Theoretical models predict that the strong UV resonance lines of C IV and O VI display distinct P Cygni wind profiles at rather low mass-loss rates while the optical absorption lines form deep in the hydrostatic layers and cannot be used for wind studies in this case. In particular, the extremely hot temperatures in the line forming regions favor the population of O VI over the (isoelectronic) C IV, because C IV is much easier ionized into its next ionization stage than O VI which has a higher ionization potential. As a consequence O VI 1032/1038Å is generally much stronger than C IV 1550Å. The C IV line has been detected in UV spectra of all five stars of our present sample, albeit very weak in K 1-16, RX J2117.1+3412, and NGC 246 (Koesterke et al. 1998). Hence it appeared useful to perform FUV observations in order to derive reliably mass-loss rates from the O VI resonance line.

2. Observations

Three targets were observed during the ORFEUS-SPAS II mission with the Berkeley spectrograph (NGC 7094, RX J2117.1+3412, Abell 78), one during the first ORFEUS-SPAS mission with the same instrument (NGC 246), and another one during the HUT-Astro 2 flight (K 1-16). Data reduction techniques for the first ORFEUS mission are described in Hurwitz & Bowyer (1995). The general design of the Berkeley spectrograph is discussed by Hurwitz & Bowyer (1986, 1996), while details concerning the calibration of the Hopkins Ultraviolet Telescope and the reduction of the K 1-16 spectrum are found in Kruk et al. (1998) and Kruk & Werner (1998), respectively. Calibration and performance for the ORFEUS-SPAS II mission are described by Hurwitz et al. (1998).

In Fig. 2 we show the three new spectra obtained during the ORFEUS-SPAS II mission. At the short wavelength end, near 912Å, the stellar flux is completely blocked by interstellar hydrogen. At the long wavelength end the blue wing of the interstellar hydrogen Lyα line is seen. All spectra show interstellar H_2 bands, most strongly visible in NGC 7094, and interstellar Lyman lines. The most prominent photospheric feature is as expected the O VI resonance line. Although not of interest in the present study we note the presence of another P Cygni line which stems from C III 977Å, and which is comparable in both strength and width to the O VI resonance line. For a systematic line identification of the weak photosphereic absorptions the reader may refer to the analysis of other PG 1159 stars by Kruk & Werner (1998).

3. Results

The wind properties of the four program stars of PG 1159-type have been recently investigated by Koesterke et al. (1998). Therefore we refer to that paper and, for a detailed description of the wind models, to Hamann & Wessolowski (1990) and Koesterke & Hamann (1997). Here we only repeat briefly the basic properties of the wind models: Spherically symmetric outflow, homogeneity and stationarity of the wind; co-moving frame radiation transfer; non-LTE conditions accounting for complex model atoms with 186 levels; usual beta-law with $\beta = 0.4$ for the velocity field.

For each of the program stars several individual wind models with varied mass-loss rates have been calculated to achieve a spectral fit to the O VI resonance line. Stellar parameters have been taken either from static plane-parallel analyses or, in case of Abell 78, from analyses based on static *and* expanding models. In this work the mass-loss rates are determined from the P Cygni profiles of the resonance lines. The spectra and the synthetic O VI profiles are shown in Fig. 3. We note that the profiles of the C III resonance line at 977 Å (not shown) are not matched by the models. One might hope that the consideration of the clumpiness of the atmospheres would overcome this problem, but there is no study dealing with more than one component available so far.

A summary of the results is included in Table 1. The mass-loss rates derived from C IV 1550 Å are also given. As already stated by Koesterke et al. (1998) for three stars (NGC 7094, K 1-16, and RX J2117.1+3412) these values are not consistent and the two values differ by factors of two and more. The reason for this remains unclear. Both ions are members of the same isoelectric sequence and both lines are emitted in the same region of the atmosphere. One possible solution, decreasing the oxygen abundance by the factor between the two values of the mass-loss rates, is in strict contradiction to the oxygen abundance derived from the plane-parallel analyses. Alternatively one might attribute the problem to the temperature stratification of the model atmospheres. Currently the temperature is consistently solved together with the non-LTE statistical equilibrium equations but, because the iron line blanketing is not accounted for, the cooling of iron lines is also neglected. It is conceivable that, due to the different ionization potentials of C IV and O VI, a change of the temperature might have different effects on the strength of both lines, but at the moment this point cannot be discussed quantitatively. Also the striking fact that for two stars (NGC 246 and Abell 78) the strengths of the resonance lines are consistently matched by one mass-loss rate would remain entirely unsolved. We state that the exact value of the mass-loss rate is at best known within a factor of 2. Additionally one might speculate that the C III resonance line, which is observed but not reproduced by the models yet, is formed in the outer layers of the atmospheres if the cooling by iron lines is accounted for.

In the following a few comments on the individual objects are given.

Abell 78 We have previously performed a detailed spectral analysis of this [WC]–PG 1159 transition object (Werner & Koesterke 1992). In that first attempt to determine wind characteristics of hot H-deficient post-AGB stars we obtained from emission features in optical spectra as well as P Cygni profiles in high resolution IUE spectra the rate $\log(\dot{M}/\mathrm{M}_{\odot}\mathrm{yr}^{-1}) = -7.6$. Taking over the atmospheric parameters of our previous work we present here a slightly improved value of $\log(\dot{M}/\mathrm{M}_{\odot}\mathrm{yr}^{-1}) = -7.3$, which is within the error range of our first analysis.

K 1-16 A high-resolution HST spectrum shows a very shallow C IV P Cygni profile and it was utilized by Patriarchi & Perinotto (1996) to determine $\log(\dot{M}/\mathrm{M}_{\odot}\mathrm{yr}^{-1}) < -10.7$ by a fit with Sobolev models. An analysis of the same observation with detailed model atmospheres (Koesterke et al. 1998) arrived at a much higher rate, $\log(\dot{M}/\mathrm{M}_{\odot}\mathrm{yr}^{-1}) = -7.6$. The discrepant results might be due to an unrealistic assumption about the carbon ionization structure in the work of Patriarchi & Perinotto (1996). Our present fit to the O VI line confirms the high mass-loss rate of K 1-16, but it is slightly smaller, by a factor of three: $\log(\dot{M}/\mathrm{M}_{\odot}\mathrm{yr}^{-1}) = -8.1$.

RX J2117.1+3412 This is the hottest star (T_{eff}=170 kK) in our sample. Applying static models it has been analyzed previously using data from the X-ray through the optical region. Latest results were obtained utilizing high resolution HST spectra (Werner et al. 1996). A very shallow blue shifted C IV absorption – similar to K 1-16 – was used by Koesterke et al. (1998) to determine $\log(\dot{M}/\mathrm{M}_{\odot}\mathrm{yr}^{-1}) = -7.0$. Our analysis of the strong O VI profile arrives at a lower value: $\log(\dot{M}/\mathrm{M}_{\odot}\mathrm{yr}^{-1}) = -7.4$.

NGC 246 After the co-addition of nine IUE high resolution spectra (Feibelman & Johansson 1995) the shallow C IV P Cygni profile of C IV 1550Å was used by Koesterke et al. (1998) to determine $\log(\dot{M}/\mathrm{M}_{\odot}\mathrm{yr}^{-1}) = -6.9$. Our present analysis of the O VI line arrives at the very same value.

NGC 7094 As already mentioned, this PG 1159 star is one of only four objects sub-classified as "hybrid", because it shows hydrogen Balmer lines in the optical spectrum in addition to the usual PG 1159 features. As a unique feature among this quartet of stars, NGC 7094 shows a prominent P Cygni profile of the C IV resonance line and Koesterke et al. (1998) found $\log(\dot{M}/\mathrm{M}_{\odot}\mathrm{yr}^{-1}) = -7.3$. Our present analysis exploiting the O VI line profile again leads to a slightly lower value: $\log(\dot{M}/\mathrm{M}_{\odot}\mathrm{yr}^{-1}) = -7.7$.

4. Mass-loss mechanism

We compare our results with predictions of the radiation driven wind theory. As expected from the weak P Cygni profiles in the UV and the pure absorption spectrum in the optical, the mass-loss rate of K 1-16 is smaller than that of the transition object Abell 78. Note that K 1-16 is most suitable for a comparison because it is very similar in mass, luminosity and chemical composition to the [WCE] and [WC]-PG 1159 stars. NGC 7094 has a remarkable amount of hydrogen while both other PG 1159 stars are more massive and therefore more luminous.

The strengths of the mass-loss and the velocities of the winds of the four PG 1159 stars in our sample are nicely in accordance with the predictions of Pauldrach et al. (1988), who investigated the properties of radiation driven winds for hot CSPN from a theoretical point of view. Although their model grids up to 100 kK do not cover the temperature of our program stars, the principal effect of stellar mass and chemical composition on the terminal velocity and the mass-loss rate can be studied. As predicted the more massive stars (NGC 246 and RX J2117.1+3412) have higher mass-loss rates and slightly lower terminal velocities than K 1-16. Also the terminal velocity of the hybrid star NGC 7094 is slightly lower and its mass-loss rate is slightly enhanced, compared to K 1-16. In order to compare absolute values, we extrapolate the results for extreme helium atmospheres of Pauldrach et al. (1988, their Fig. 6b) to 140 kK ($M = 0.645\,\mathrm{M}_{\odot}$) and read off $\dot{M} \approx 10^{-8}\,\mathrm{M}_{\odot}\,\mathrm{yr}^{-1}$ which is almost the same value as derived from the O VI line of K 1-16. Note that this extrapolation should not be overinterpretated, especially since the line list used by Pauldrach et al. (1988) is incomplete for $T_{\mathrm{eff}} > 50000\,\mathrm{K}$.

Koesterke et al. (1998) also considered the strong mass-loss of the [WCE] stars. The ratio between the mechanical wind momentum and the momentum of the radiation field ($\eta = \frac{\dot{M} v_\infty}{Lc}$) differs considerably for [WCE] and PG 1159 stars and, in case of the [WCE] stars, exceeds unity by far. Following Lucy & Abbott (1993), they speculated that the mass-loss is enhanced due to multi-scattering processes induced by changes in the degree of ionization, simply because the total number of lines is increased when different ionization stages are dominant in different depths. The photons are scattered by lines of high ionization stages close to the star *and* again scattered by lines of low stages further out in the wind. This assumption was supported by the fact that the degree of ionization of oxygen does change in Sand 3, a typical [WCE] star, but does not change in K 1-16, a typical PG 1159 star. In the present work we corroborate this hypothesis and present the ionization stratifications of Sand 3 and K 1-16 together with that of Abell 78, the transition object of [WC]-PG 1159 type (Fig. 4). As expected there is, in contrast to K 1-16, a change of ionization in the continuum forming part of Abell 78 ($\tau_{\mathrm{Ross}} = 0.1 \ldots 10$), but it seems to be not that steep as in Sand 3.

To summarize, the following picture about the mass-loss history during the hot post-AGB stages of hydrogen-deficient stars emerges. Possibly as a consequence of a late helium shell flash, a star leaves the AGB with a H-deficient atmosphere. It evolves through the [WC] stage, heating up to effective temperatures of about T_{eff}=140 kK at almost constant luminosity. Throughout this evolutionary stage stratified ionization structures within the atmosphere maintain high mass-loss rates due to multi-scattering processes. As a consequence we observe strong optical and UV emission lines. During the subsequent evolution T_{eff} increases to an extent that no recombination in the outer photospheric layers occurs any longer. Multi-scattering of photons ceases and the mass-loss rate is reduced to a strength as predicted by radiation driven wind theory with $\eta \approx 1$. The star now appears as a PG 1159 star with optical absorption lines and P Cygni features in the UV. During further evolution the luminosity decreases and mass-loss is turned down to an unobservable extent when the star enters the hot end of the white dwarf cooling sequence.

ORFEUS data analysis in Tübingen is supported by the DLR under grant 50 QV 97054.

REFERENCES

Blöcker T. 1995, A&A, 299, 755

Dreizler S., Werner K., Heber U. 1995 in "White Dwarfs", D. Koester and K. Werner (eds), Lecture Notes in Physics, Springer-Verlag, p. 160

Feibelman, W.A., & Johansson, S. 1995, ApJS, 100, 405

Hamann, W.-R. 1997, in Planetary Nebulae, IAU Symp. 180, H.J. Habing and H.J.G.L.M. Lamers (eds.), in press

Hamann W.-R., Wessolowski U. 1990, A&A, 227, 171

Hurwitz, M., & Bowyer, S. 1986, Proc. SPIE, 627, 375

Hurwitz, M., & Bowyer, S. 1995, ApJ, 446, 812

Hurwitz, M., & Bowyer, S. 1996, in Astrophysics in the Extreme Ultraviolet, S.Bowyer and R.F.Malina (eds.), Dordrecht: Kluwer, p. 601

Hurwitz, M., et al. 1998, ApJ, this issue

Koesterke L., Hamann W.-R. 1997, A&A, 320, 91

Koesterke, L., Dreizler, S., & Rauch, T. 1998, A&A, 330, 1041

Kruk, J.W., & Werner, K. 1998, ApJ, submitted

Kruk, J.W., Finley, D.S., & Kriss, G.A. 1998, in preparation

Lucy L.B., Abbott D.C. 1993, ApJ, 405, 738

Patriarchi P., & Perinotto M. 1996, A&A, 309, 895

Pauldrach, A., Puls, J., Kudritzki, R.P., Méndez, R.H., Heap, S.R. 1988, A&A, 207, 123

Rauch, T., & Werner, K. 1997, in The Third Conference on Faint Blue Stars, A.G.D. Philip, J. Liebert, R.A. Saffer (eds.), L.Davis Press, Schenectady, NY, in press

Werner, K., & Koesterke, L. 1992, in Atmospheres of Early-Type Stars, U. Heber and C.S. Jeffery (eds.), Lecture Notes in Physics 401, Springer, Berlin, p. 288

Werner, K., Dreizler, S., Heber, U., Rauch, T., Fleming, T.A., Sion, E.M., & Vauclair, G. 1996, A&A, 307, 860

Werner, K., Dreizler, S., Heber, U., Kappelmann, N., Kruk, J., Rauch, T., & Wolff, B. 1997, in Reviews in Modern Astronomy 10, R.E. Schielicke (ed.), Astronomische Gesellschaft Hamburg, p. 219

Wood, P.R., & Faulkner, D.J. 1986, ApJ, 307, 659

This manuscript was prepared with the AAS LaTeX macros v4.0.

Fig. 1.— Location of PG 1159 stars (program stars: filled symbols) in the $\log T_{\rm eff}$–$\log g$ diagram. Evolutionary tracks for He-burning post-AGB stars are from Wood & Faulkner (1986).

Fig. 2.— FUV spectra of three of the sample stars obtained during the ORFEUS-SPAS II mission. Most prominent photospheric features are P Cygni shaped line profiles of C III 977Å and O VI 1032/1038Å. Original data were smoothed with a Gaussian with 1Å FWHM. For better presentation the spectra of Abell 78 and RX J2117.1+3412 were normalized to the flux of NGC 7094 at 1150Å (scaling factor given in panel) and then shifted vertically. Horizontal lines denote the zero flux level of the respective spectrum.

Fig. 3.— Profile fits to the O VI resonance line of our five sample stars.

Fig. 4.— Ground-level non-LTE occupation numbers for the oxygen ions versus the heavy particle density of the final models of Sand 3 (top), Abell 78 (middle) and K 1-16 (bottom).

Table 1: Summary of the model parameters. Two different values for the mass-loss rates are given with respect to the C IV and the O VI line. The stellar masses and luminosities are derived by comparison with evolutionary tracks by Blöcker (1995).

		static analyses									wind analyses		
Star	type[a,c]	T_*	$\log g$	H	He	C	O	N	$\log L$	M	$\log \dot{M}$		v_∞
		[kK]	[cgs]	mass fraction					$[L_\odot]$	$[M_\odot]$	$[M_\odot\ \mathrm{yr}^{-1}]$		[km/s]
											C IV	O VI	
NGC 7094[a]	lgEH	110	5.7	42	51	5	<1	<1	3.6	0.63	-7.3	-7.7	3500
K 1-16[a]	lgE	140	6.1		38	56	6		3.6	0.63	-7.6	-8.1	4000
NGC 246[b]	lgE	150	5.7		64	30	6		4.2	0.84	-6.9	-6.9	3500
RXJ2117.1+3412[b]	lgE	170	6.0		33	50	17		4.2	0.83	-7.0	-7.4	3500
Abell 78[c]	[WC]-PG 1159	110	5.5		35	50	15		3.7	0.77	-7.3	-7.3	3750

[a]Dreizler et al. (1995); [b]Rauch & Werner (1997); [c]Werner & Koesterke (1992)

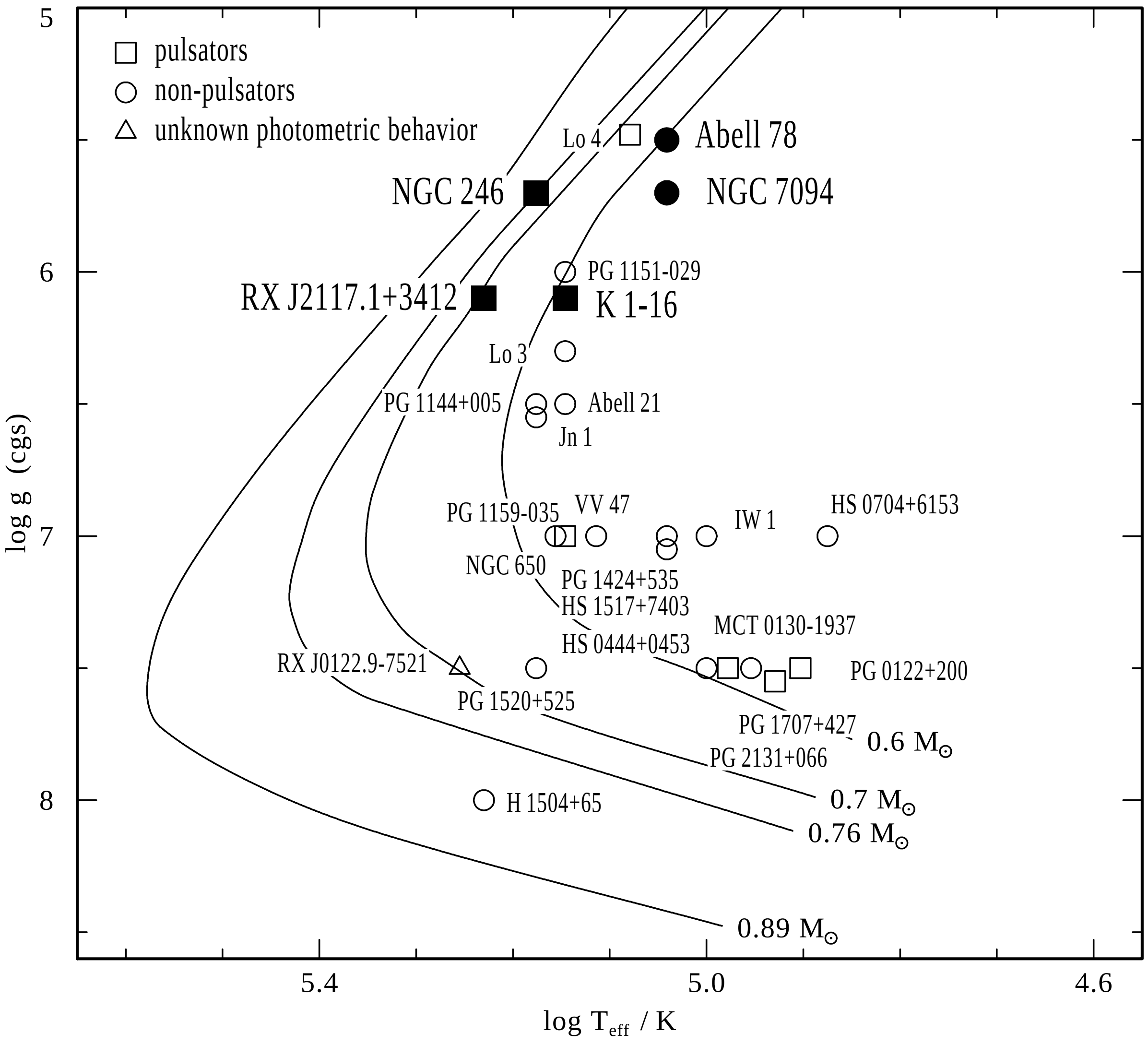
pulsators
non-pulsators
unknown photometric behavior
Lo 4
Abell 78
NGC 246
NGC 7094
PG 1151-029
RX J2117.1+3412
K 1-16
Lo 3
PG 1144+005
Abell 21
Jn 1
PG 1159-035
VV 47
IW 1
HS 0704+6153
NGC 650
PG 1424+535
HS 1517+7403
MCT 0130-1937
HS 0444+0453
RX J0122.9-7521
PG 0122+200
PG 1520+525
PG 1707+427
0.6 $M_\odot$
PG 2131+066
0.7 $M_\odot$
H 1504+65
0.76 $M_\odot$
0.89 $M_\odot$
5
6
7
8
log g (cgs)
5.4
5.0
4.6
log T_{eff} / K

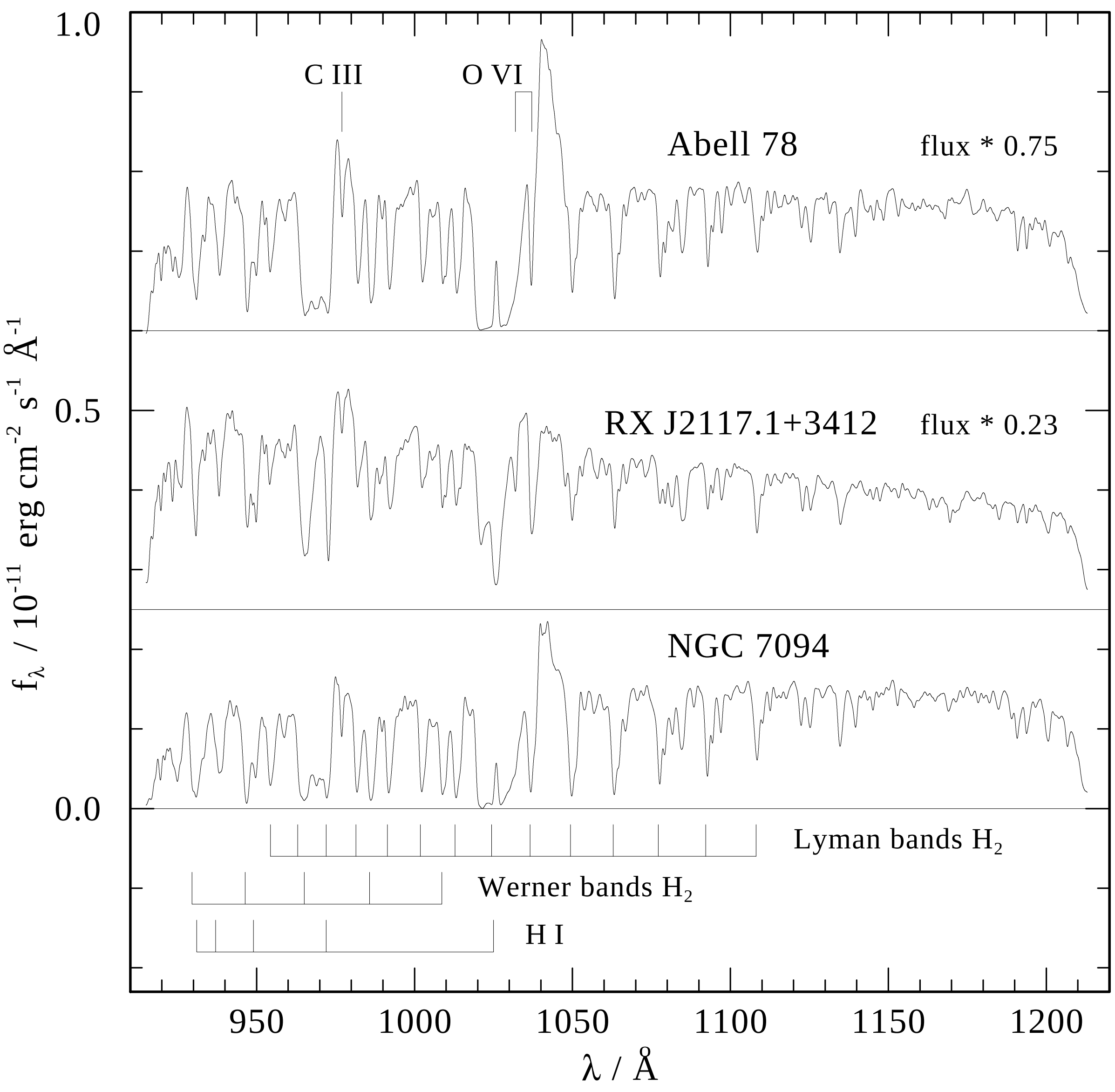

1.0
0.5
0.0
C III
O VI
Abell 78
flux * 0.75
RX J2117.1+3412
flux * 0.23
NGC 7094
Lyman bands H_2
Werner bands H_2
H I
f_λ / 10^{-11} erg cm^{-2} s^{-1} Å^{-1}
950
1000
1050
1100
1150
1200
λ / Å

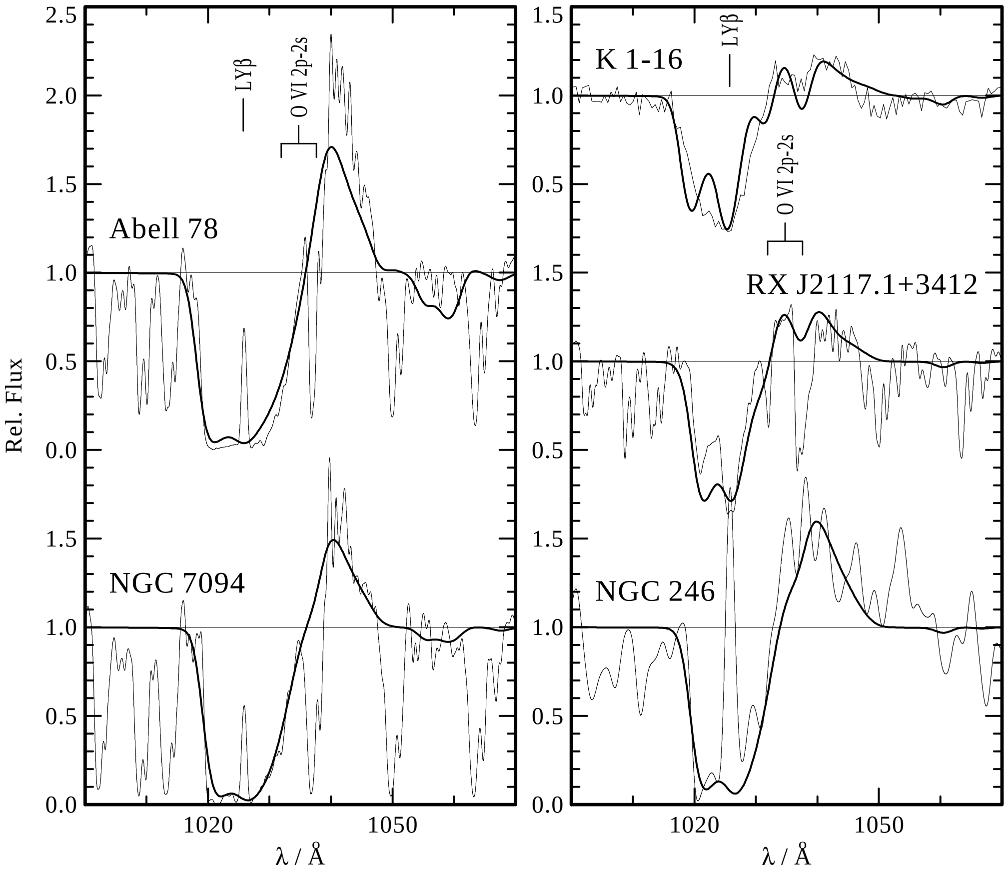
Abell 78
NGC 7094
K 1-16
RX J2117.1+3412
NGC 246
LYβ
O VI 2p-2s
Rel. Flux
λ / Å
1020
1050

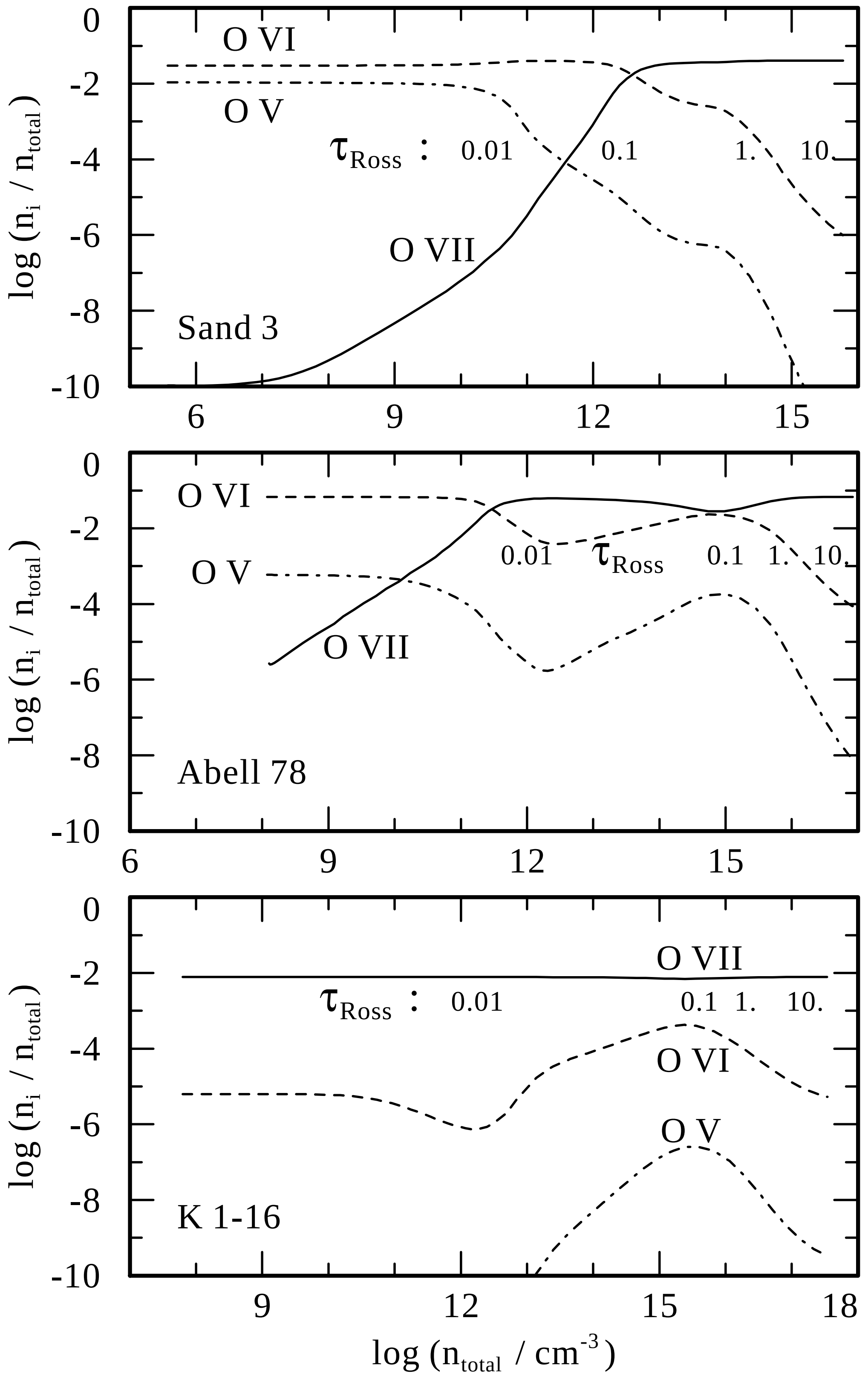
O VI
O V
O VII
τ_{Ross} : 0.01 0.1 1. 10.
Sand 3
log (n_i / n_{total})
0
-2
-4
-6
-8
-10
6
9
12
15
O VI
O V
O VII
0.01 τ_{Ross} 0.1 1. 10.
Abell 78
log (n_i / n_{total})
6
9
12
15
O VII
τ_{Ross} : 0.01 0.1 1. 10.
O VI
O V
K 1-16
log (n_i / n_{total})
9
12
15
18
log (n_{total} / cm^{-3})